# Electronic Supplementary Information

## Direct observation of *o*-benzyne formation in photochemical hexadehydro-Diels–Alder (*hν*-HDDA) reactions

Xiaonan Ma,[a,b] Jan Maier,[c] Michael Wenzel,[a] Alexandra Friedrich,[c] Andreas Steffen,[c,d] Todd B. Marder,[c,*] Roland Mitrić,[a,*] Tobias Brixner[a,*]

[a] Institut für Physikalische und Theoretische Chemie, Universität Würzburg, Am Hubland, 97074 Würzburg, Germany

[b] Institute of Molecular Plus, Tianjin University, No. 92 Weijin Road, Nankai District, 300072 Tianjin, China

[c] Institut für Anorganische Chemie, and Institute for Sustainable Chemistry & Catalysis with Boron, Universität Würzburg, Am Hubland, 97074 Würzburg, Germany

[d] Institut für Anorganische Chemie, Technische Universität Dortmund, Otto-Hahn-Str.6, 44227 Dortmund, Germany

*** Corresponding author:**

**todd.marder@uni-wuerzburg.de**

**roland.mitric@uni-wuerzburg.de**

**brixner@uni-wuerzburg.de**

## Table of Contents

**Note 1: General information on chemical synthesis and isolation**

Unless otherwise noted, all reactions were performed using standard Schlenk techniques under argon. HPLC grade solvents were argon saturated, dried using an Innovative Technology Inc. Pure-Solv Solvent Purification System, and further deoxygenated by using the freeze-pump-thaw method. Me-BD-Me was synthesized according to the procedure we have reported.[1] Starting materials were purchased from commercial sources and used without further purification. Automated flash chromatography was performed using a Biotage® Isolera Four system on silica gel (Biotage® SNAP cartridge KP-Sil 10 g, KP-Sil 25 g and HP-Sil 50 g). Commercially available, precoated TLC plates (Polygram® Sil G/$UV_{254}$ and Polygram® Alox N/$UV_{254}$) were purchased from Machery-Nagel. The removal of solvent was performed on a rotary evaporator *in vacuo* at a maximum temperature of 45 °C.

Elemental analysis was performed in the Institute of Inorganic Chemistry, Universität Würzburg on an Elementar vario MICRO cube elemental analyzer. High resolution mass spectra were obtained using a Thermo Fisher™ Scientific Exactive Plus Orbitrap MS System with an Atmospheric Sample Analysis Probe (ASAP) or with Atmospheric Pressure Chemical Ionization (APCI).

All NMR spectra were recorded at ambient temperature using a Bruker Avance 500 NMR ($^1$H, 500 MHz; $^{13}$C{$^1$H}, 125 MHz) spectrometer. $^1$H NMR chemical shifts are reported relative to residual proton resonances of the corresponding deuterated solvent ($CDCl_3$: 7.26 ppm; $CD_2Cl_2$: 5.32 ppm) whereas $^{13}$C{$^1$H} NMR spectra are reported relative to the carbon signals of the deuterated solvent ($CDCl_3$: 77.16 ppm; $CD_2Cl_2$: 53.84 ppm).

A crystal suitable for single-crystal X-ray diffraction was selected, coated in perfluoropolyether oil, and mounted on a MiTeGen sample holder. Diffraction data of Me-$H_2$BZ-Me were collected on a RIGAKU OXFORD DIFFRACTION XtaLAB Synergy diffractometer with a semiconductor HPA-detector (HyPix-6000) and multi-layer mirror monochromated Cu-$K_\alpha$ radiation. The crystal was cooled using an Oxford Cryostream 800 low-temperature device. Data were collected at 100 K. The images were processed and corrected for Lorentz-polarization effects and absorption (empirical scaling) as implemented in the CrysAlis$^{Pro}$ software. The structure was solved using the intrinsic phasing method[2] (ShelXT) and Fourier expansion technique. All non-hydrogen atoms were refined in anisotropic approximation, with hydrogen atoms 'riding' on idealised positions by full-matrix least squares against $F^2$ of all data, using SHELXL software[3] and the SHELXLE graphical user interface.[4] Crystal data and experimental details are listed in Table S1; full structural information has been deposited with the Cambridge Crystallographic Data Centre. CCDC-1990248.

Static UV-visible absorption measurements were performed in standard quartz cuvettes (1 cm x 1 cm cross-section). Absorption spectra were recorded using an Agilent 8453 diode array UV-visible spectrophotometer at room temperature in HPLC grade solvents, which were further purified and dried by using an Innovative Technology Inc. Pure-Solv Solvent Purification System.

## References

1. J. Maier, M. Deutsch, J. Merz, Q. Ye, O. Diamond, M.-T. Schilling, A. Friedrich, B. Engels and T. B. Marder, *Submitted for publication.*

2. G. M. Sheldrick, *Acta Crystallogr. A Found. Adv.* 2015, **71**, 3–8.

3. G. M. Sheldrick. *Acta Crystallogr. A Found. Crystallogr.* 2008, **64**, 112–122.

4. C. B. Hübschle, G. M. Sheldrick and B. Dittrich, *J. Appl. Crystallogr.* 2011, **44**, 1281–1284.

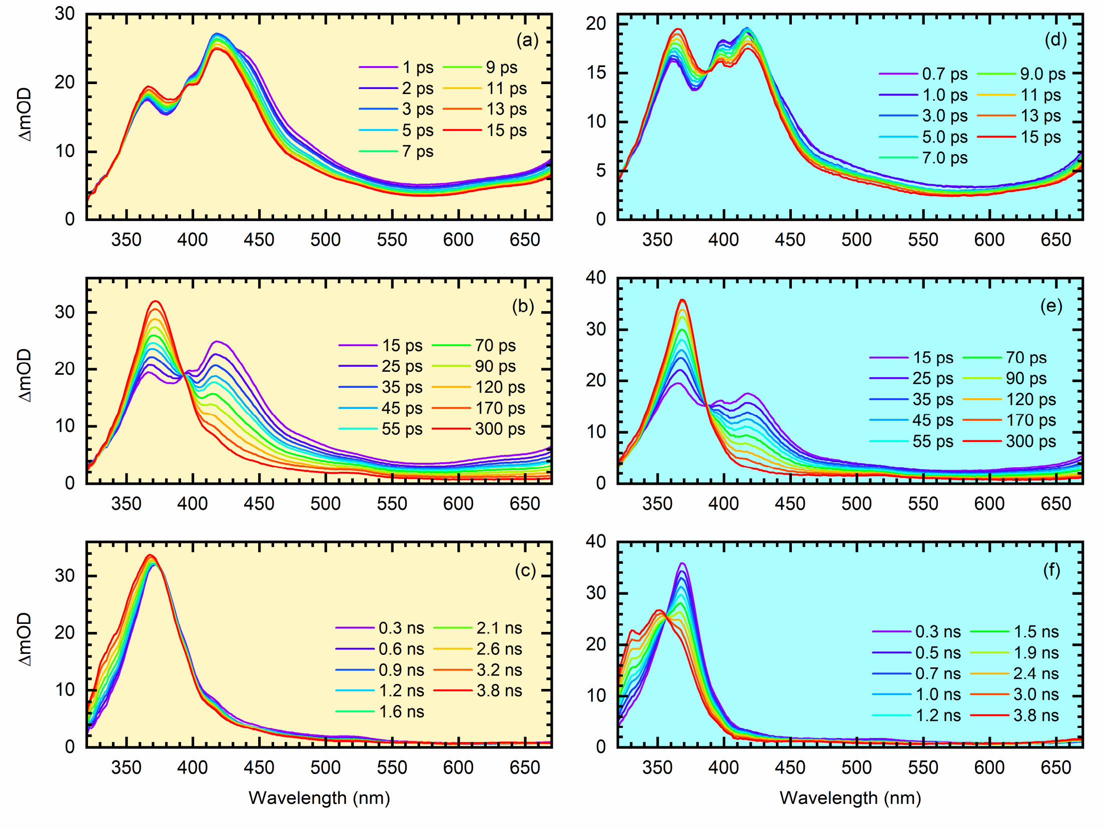

**Figure S1. Transient UV/VIS absorption spectra of Me-BD-Me in 320-670 nm regime.** Data are shown for Me-BD-Me dissolved in $CHCl_3$ (a–c, left column, yellow background) and $CH_3CN$ (d–f, right column, cyan background) upon photoexcitation at 295 nm in the delay ranges of (a, d) 500 fs to 15 ps, (b, e) 15 ps to 300 ps, and (c, f) 300 ps to 3.8 ns.

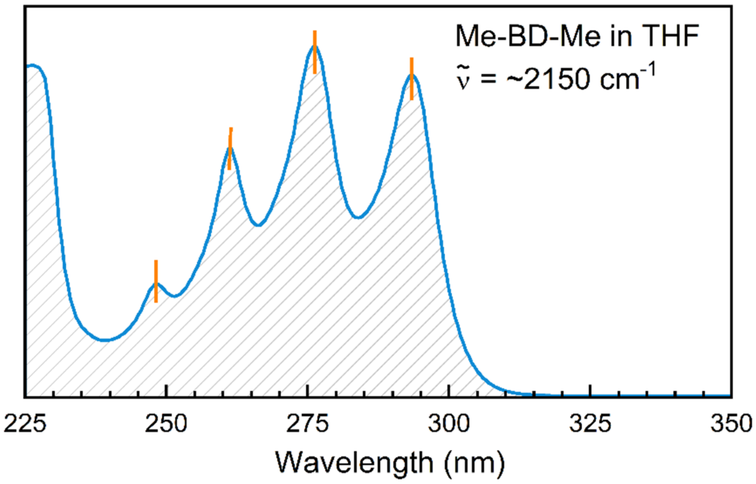

**Figure S2. Static UV/VIS absorption spectrum of Me-BD-Me in THF.** The first absorption band (250–330 nm) shows a clear vibronic progression (marked in orange) with vibrational frequency of ~2150 cm$^{-1}$, which corresponds to the pronounced –C≡C– stretching mode of bis-diynes.

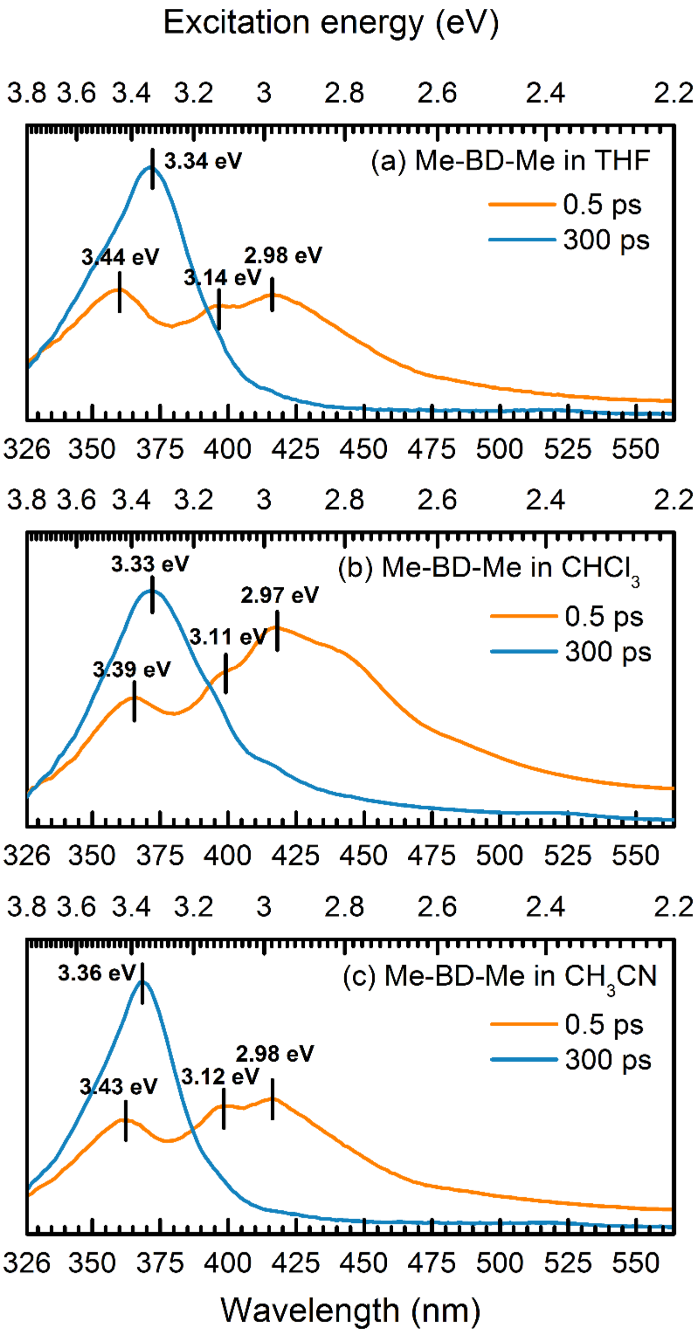

**Figure S3. Transient absorption spectra at a delay of 0.5 ps (orange line) and 300 ps (blue line) of Me-BD-Me.** Data are shown for **a,** in THF, **b,** in $CHCl_3$, and **c,** in $CH_3CN$. The corresponding vertical excitation energies (in eV) of each absorption peak are also marked.

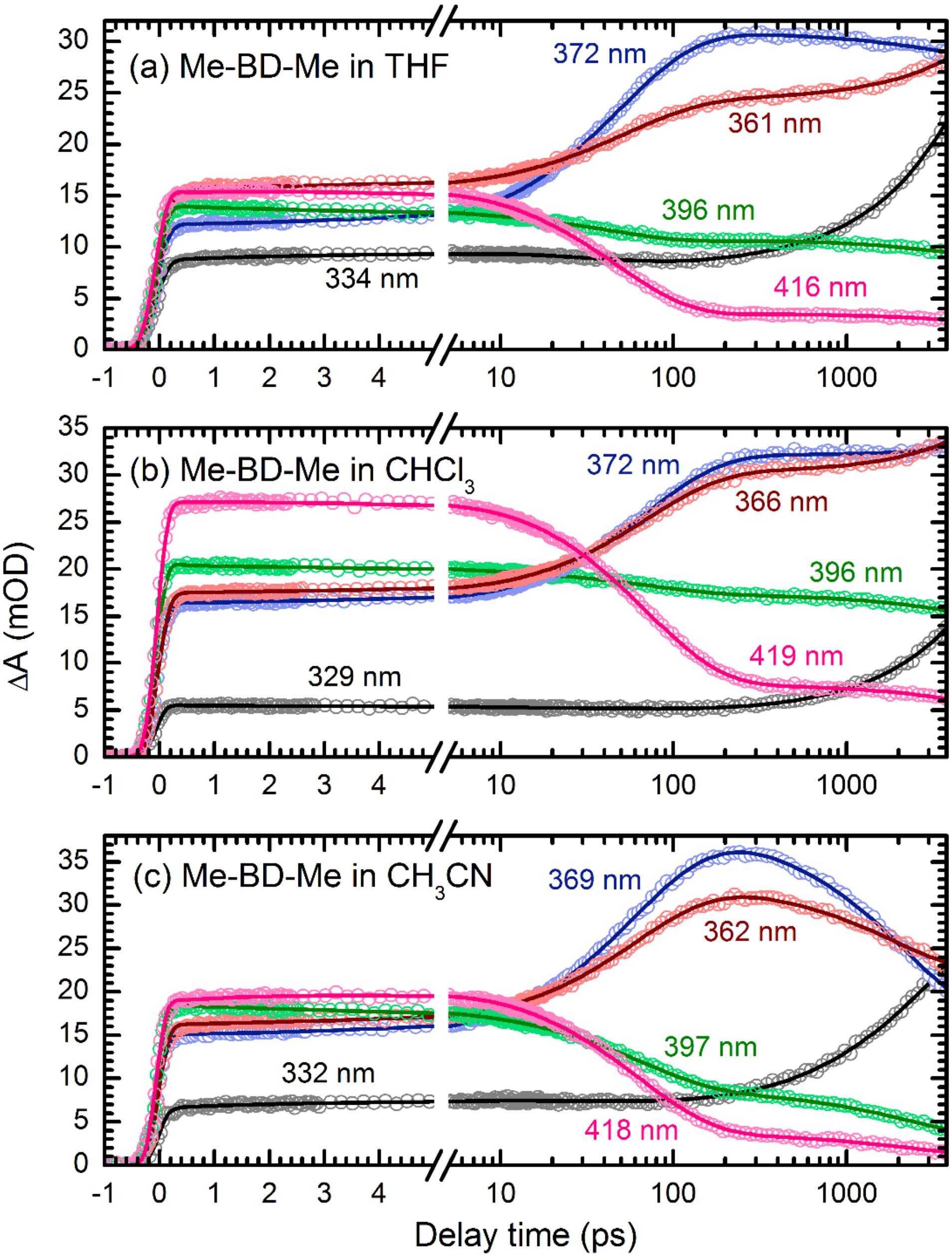

**Figure S4. Target analysis (colored lines) in comparison with experimental transients (unfilled circles) of Me-BD-Me at selected probe wavelengths.** The UV-induced transient absorption time traces are shown for experiments **a,** in THF, **b,** in $CHCl_3$, and **c,** in $CH_3CN$.

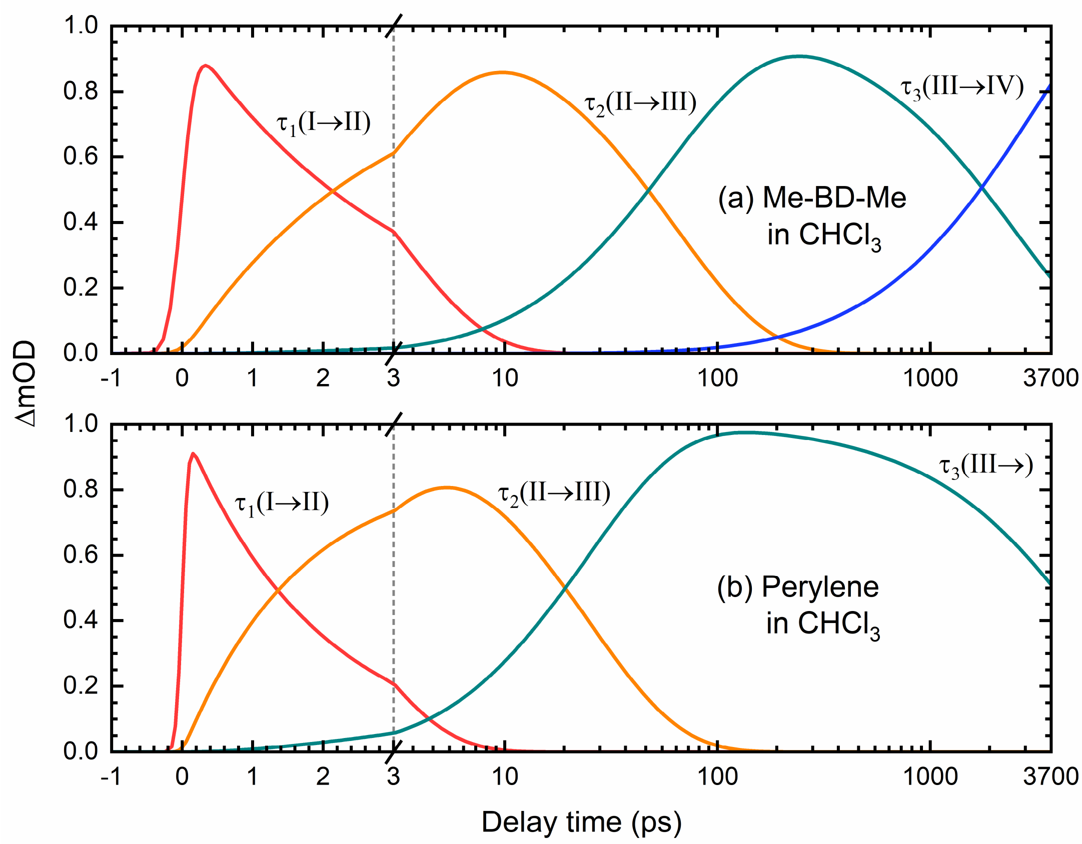

**Figure S5. Target analysis fitted concentration evolution of each transient species of Me-BD-Me (a) and perylene (b) in $CHCl_3$.**

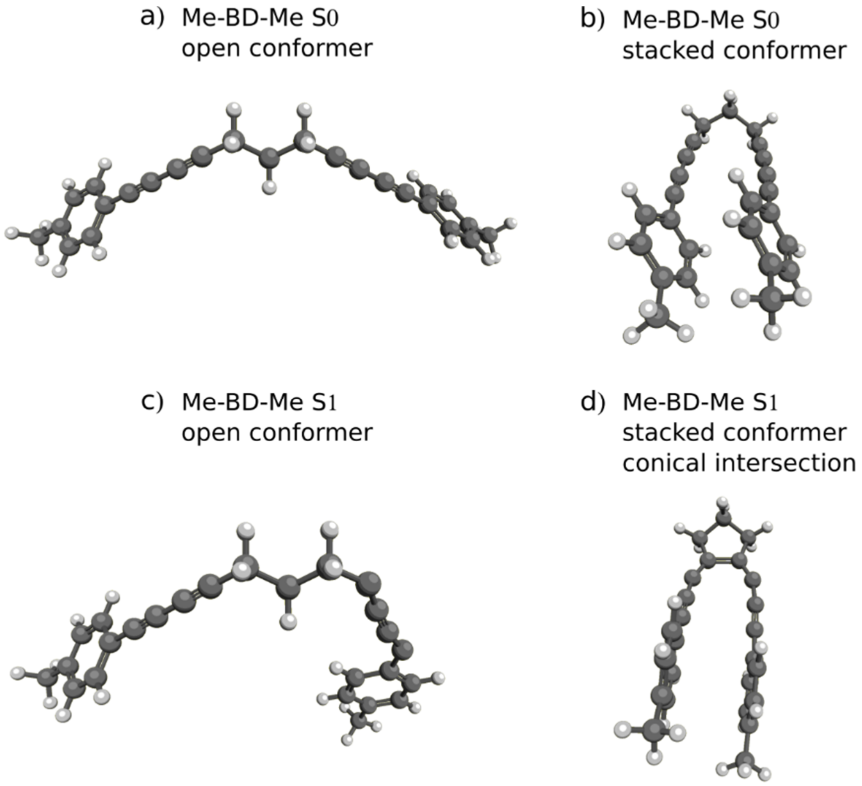
a) Me-BD-Me S0 open conformer

b) Me-BD-Me S0 stacked conformer

c) Me-BD-Me S1 open conformer

d) Me-BD-Me S1 stacked conformer conical intersection

**Figure S6. Optimized structures of Me-BD-Me for $S_0$ and $S_1$ states.** All geometries are optimized by using the CAM-B3LYP functional in combination with the def2-TVZP basis set including solvent effects of THF *via* the PCM model and empirical dispersion correction GD3BJ. **a,** Singlet ground-state ($S_0$) structure of open conformer. **b,** Singlet ground-state ($S_0$) structure of stacked conformer. **c,** First singlet-excited-state ($S_1$) structure of open conformer. **d,** First singlet-excited-state ($S_1$) structure of stacked conformer. All structures were optimized to the global minimum of the potential energy surface, *i.e.*, no imaginary frequencies were found except for structure **d,** for which a degeneracy of $S_0$ and $S_1$ is observed.

## Note 2: Synthesis of 5-(p-tolyl)-4-(p-tolylethynyl)-2,3-dihydro-1*H*-indene (Me-$H_2$BZ-Me)

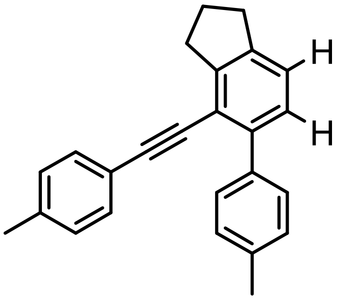

The compound **Me-BD-Me** (264 mg; 0.77 mmol) was dissolved in 40 mL of cyclooctane and stirred for 2 days at 140 °C. After removal of cyclooctane *in vacuo*, the reaction mixture was purified using flash chromatography with cyclohexane as eluent. The solvent of the first fraction was evaporated and the crude product was recrystallized from dichloromethane/hexane over night at -30 °C to give **Me-$H_2$BZ-Me** as an off-white solid. Yield: 130 mg (49%).

**$^1$H NMR** (500 MHz, $CD_2Cl_2$, r.t., ppm) δ: 7.58-7.56 (m, 2 H, CH), 7.28-7.24 (m, 5 H, CH), 7.20 (m, 1 H, CH), 7.15-7.13 (m, 2 H, CH), 3.14 (t, *J* = 7 Hz, 2 H, $CH_2$), 3.00 (t, *J* = 7 Hz, 2 H, $CH_2$), 2.42 (s, 3 H, $CH_3$), 2.35 (s, 3 H, $CH_3$), 2.16 (quin., *J* = 7 Hz, 2 H, $CH_2$).

**$^{13}$C{$^1$H} NMR** (125 MHz, $CD_2Cl_2$, r.t., ppm) δ: 148.2 ($C_q$), 143.3 ($C_q$), 141.6 ($C_q$), 138.9 ($C_q$), 138.4 ($C_q$), 137.4 ($C_q$), 2 x 131.5 (CH), 2 x 129.6 (CH), 2 x 129.5 (CH), 2 x 128.9 (CH), 127.9 (CH), 124.6 (CH), 121.0 ($C_q$), 118.1 ($C_q$), 95.6 ($C_q$), 87.8 ($C_q$), 33.7 ($CH_2$), 33.5 ($CH_2$), 25.3 ($CH_2$), 21.6 ($CH_3$), 21.3 ($CH_3$).

**Elem. Anal. Calc.** (%) for $C_{25}H_{22}$: C 93.12, H 6.88; found: C 92.73, H 6.98

**HRMS** (ASAP) [$C_{25}H_{22}$ + $H^+$] calc.: m/z = 323.1794; found m/z = 323.1787 (|Δ| = 2.16 ppm)

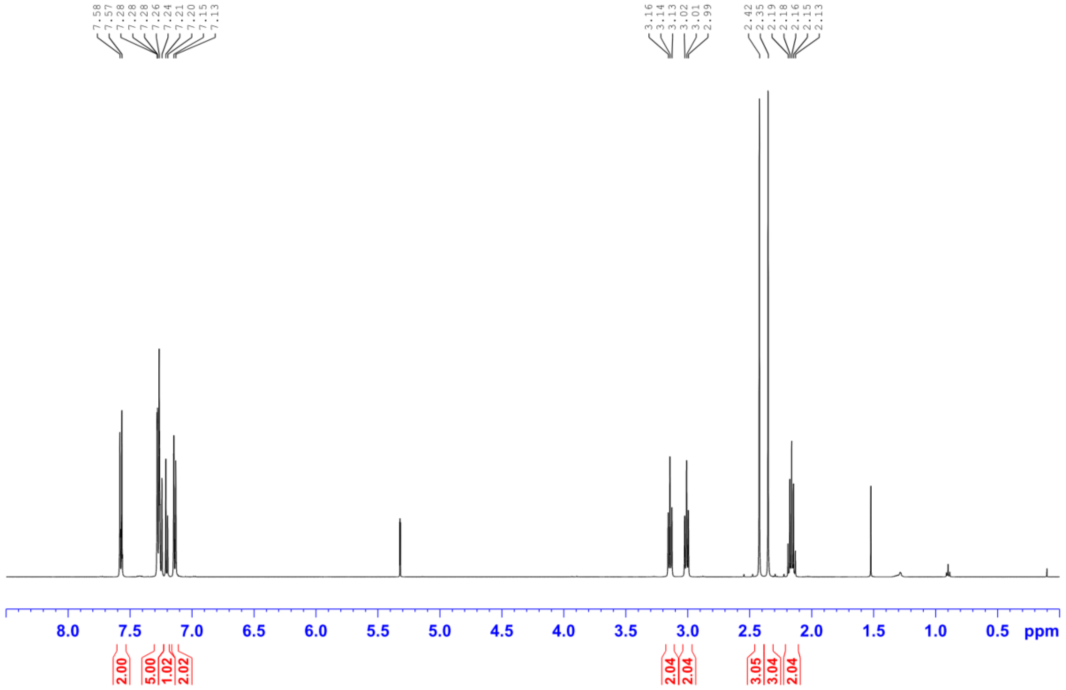

**Figure S7.** $^1$H NMR spectrum (500 MHz, $CDCl_3$) of Me-$H_2$BZ-Me.

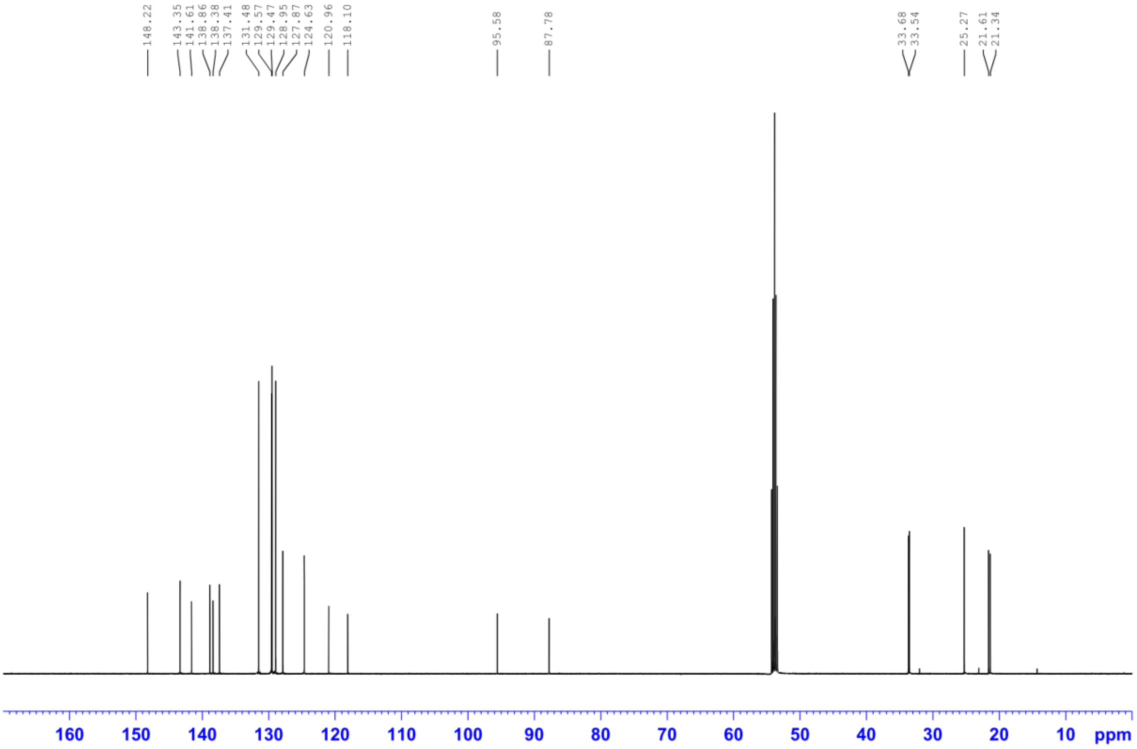

**Figure S8.** $^{13}C\{^1H\}$ NMR spectrum (125 MHz, $CDCl_3$) of Me-$H_2$BZ-Me.

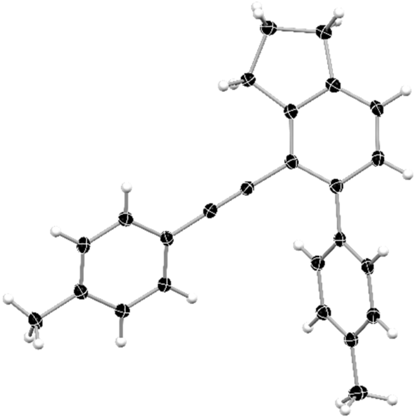

**Figure S9.** Molecular structure of Me-$H_2$BZ-Me in the solid state at 100 K. Atomic displacement ellipsoids for carbon atoms (black) are drawn at the 50% probability level, while hydrogen atoms are drawn as white balls.

**Table S1.** Single-crystal X-ray diffraction data and structure refinement of Me-$H_2$BZ-Me.

| Identification code | **Me-H$_2$BZ-Me** |
|---|---|
| CCDC number | 1990248 |
| Empirical formula | $C_{25}H_{22}$ |
| Formula weight / g·mol$^{-1}$ | 322.42 |
| $T$ / K | 100(2) |
| Radiation, $\lambda$ / Å | Cu-K$_\alpha$, 1.54184 |
| Crystal size / mm$^3$ | 0.412 × 0.261 × 0.19 |
| Crystal color, habit | colorless block |
| Crystal system | triclinic |
| Space group | $P\bar{1}$ |
| $a$ / Å | 7.48420(10) |
| $b$ / Å | 9.0245(2) |
| $c$ / Å | 13.6060(2) |
| $\alpha$ / ° | 82.5780(10) |
| $\beta$ / ° | 79.3100(10) |
| $\gamma$ / ° | 77.3810(10) |
| Volume / Å$^3$ | 877.43(3) |
| $Z$ | 2 |
| $\rho_{calc}$ / g·cm$^{-3}$ | 1.220 |
| $\mu$ / mm$^{-1}$ | 0.516 |
| $F$(000) | 344.0 |
| $\theta$ range / ° | 3.32 – 72.126 |
| Reflections collected | 14204 |
| Unique reflections | 3452 |

| | |
|---|---|
| $R_{\text{int}}$ | 0.0361 |
| $R_{\sigma}$ | 0.0276 |
| Parameters | 228 |
| GooF on $F^2$ | 1.029 |
| $R_1$ [I ≥ 2σ(I)] | 0.0421 |
| $wR_2$ [all data] | 0.1138 |
| Max. / min. residual electron density / e·Å$^{-3}$ | 0.27 / -0.24 |

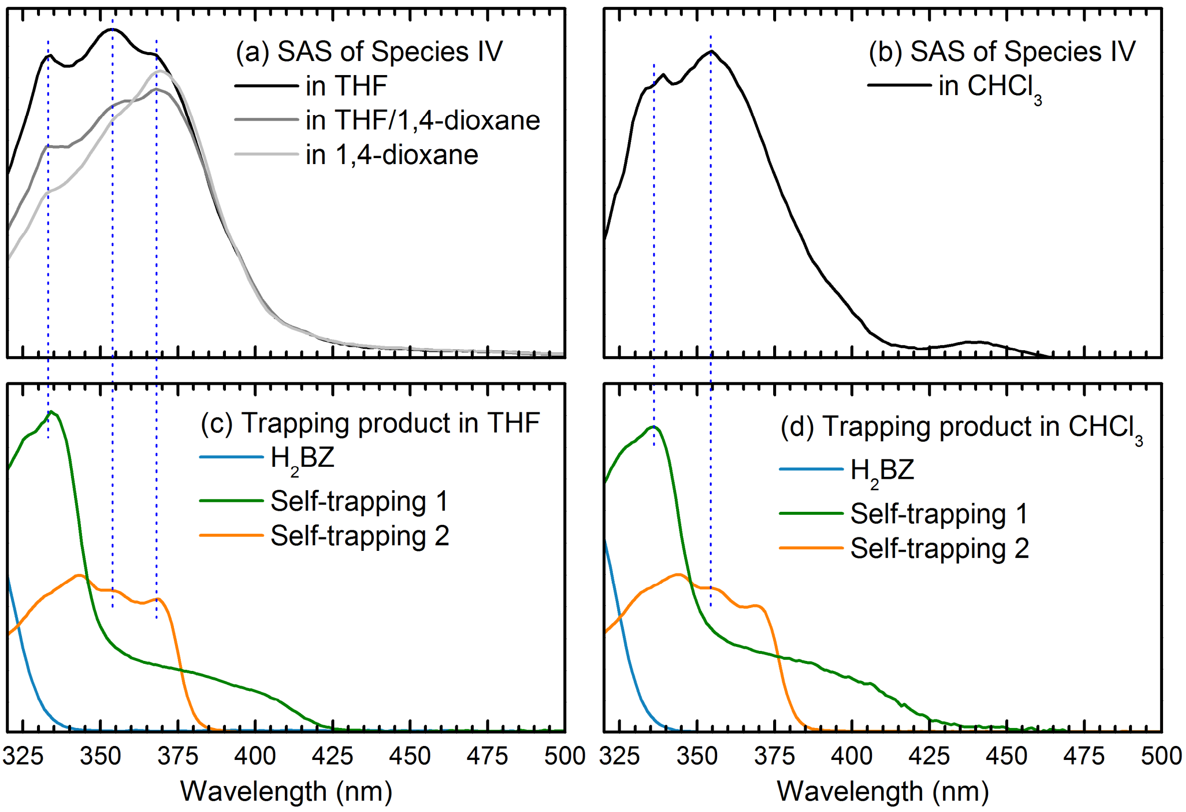

**Figure S10. Comparison between SAS of species IV from target analysis of Me-BD-Me transient absorption and measured spectra of chemically isolated trapping products. a**, SAS of species IV in THF (black), THF/1,4-dioxane (dark gray), and 1,4-dioxane (light gray). **b**, SAS of species IV in $CHCl_3$. **c,d**, Static absorption spectra of chemically isolated $H_2BZ$ (blue), species Self-trapping-1 (green) and Self-trapping-2 (orange) in THF (**c**) and $CHCl_3$ (**d**). Several dashed lines are used for assisting the comparison.

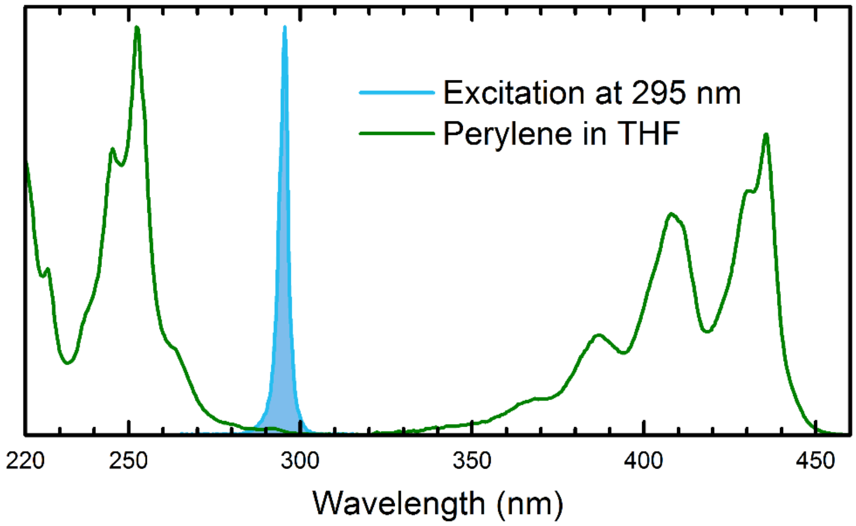

**Figure S11. Static UV/VIS absorption spectrum of perylene in THF.** The spectrum of excitation pulses (blue) employed in transient absorption experiments is centered at 295 nm and minimizes direct perylene excitation (green).

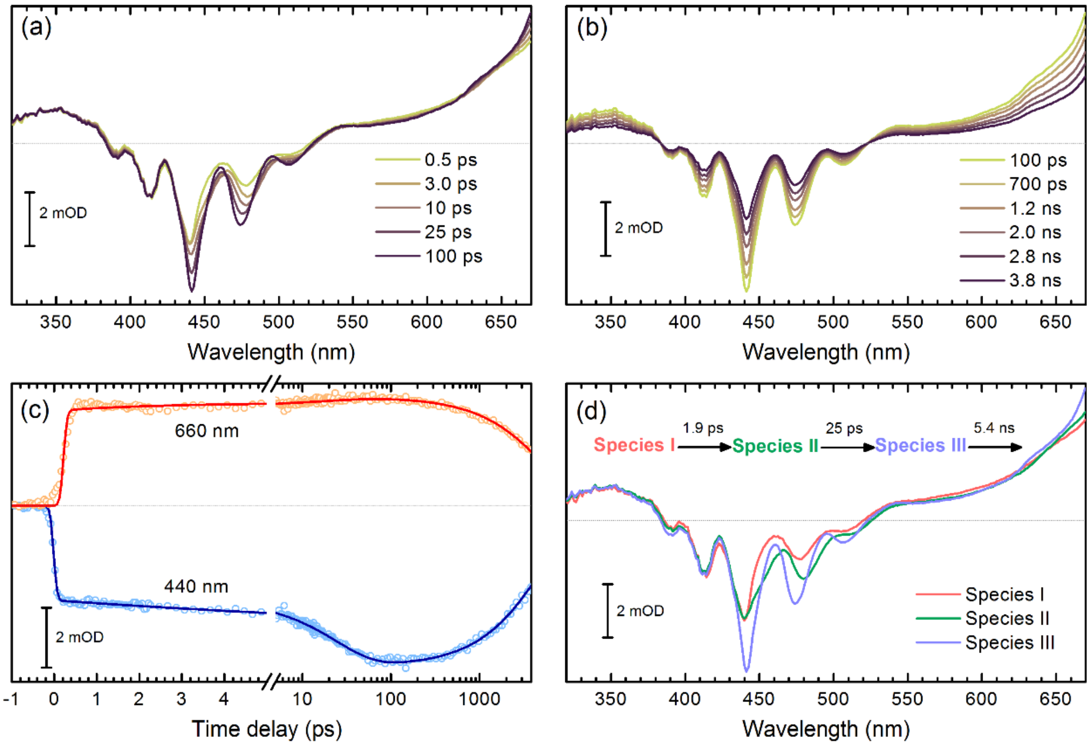

**Figure S12. Transient absorption spectra and target analysis of perylene.** The transient absorption spectra of perylene in THF are shown for **a,** 500 fs to 100 ps and **b,** 100 ps to 3800 ps. **c,** Examples of fits (solid lines) after target analysis of transient absorption data (symbols) for time traces at 440 nm and 660 nm. **d,** Species-associated spectra (SAS) from target analysis with a sequential model and corresponding fitted time constants.

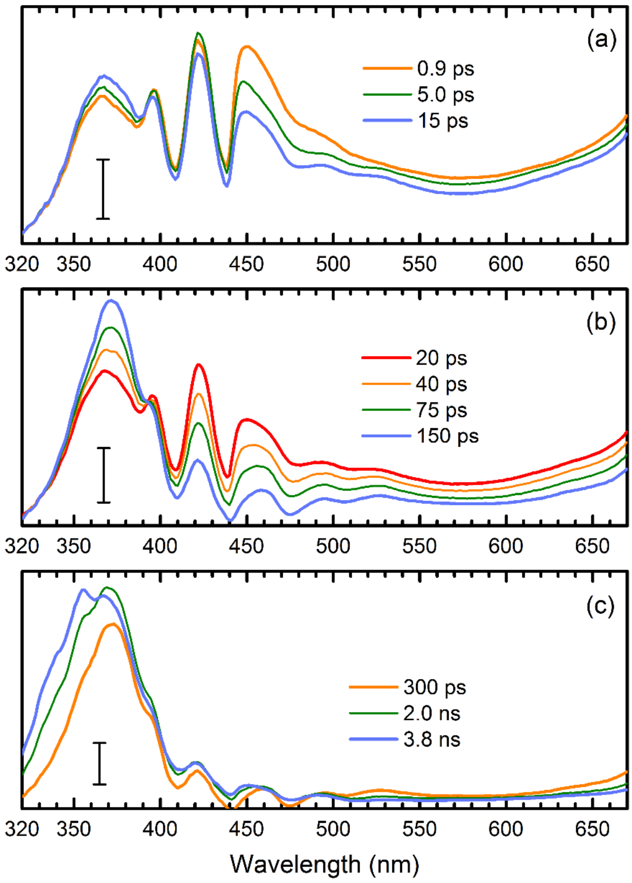

**Figure S13. Transient UV/VIS absorption spectra of a mixture of Me-BD-Me and perylene in THF.** Data are shown for delay ranges of **a,** 0.9 ps to 15 ps, **b,** 20 ps to 150 ps, and **c,** 300 ps to 3.8 ns. The scale bars correspond to an absorbance change of 5 mOD.

## Note 3: Synthesis of 14-(*p*-tolyl)-15-(*p*-tolylethynyl)-2,3-dihydro-1*H*-cyclopenta[5,6]naphtha-[1,2,3,4-*ghi*]perylene

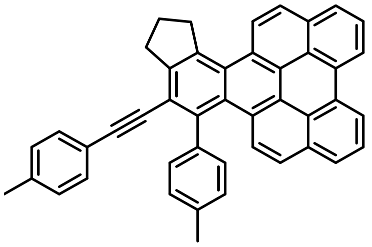

The compound **Me-BD-Me** (200 mg; 0.62 mmol) was dissolved in 4 mL chloroform and 1.5 eq. of perylene (238 mg; 0.93 mmol) were added. The mixture was stirred for 4.5 h at 150 °C in a microwave reactor. The reaction product showed poor solubility in chloroform and floated on top of the reaction mixture. After removing the solvent with a pipette, the bright yellow product was first washed with 3 x 1 mL of dichloromethane and then with 3 x 1 mL of *n*-hexane. Residual perylene still present in the crude product was removed *via* Kugelrohr distillation giving **Me-BZ-Me+P**. Yield: 50 mg (14%).

**$^1$H NMR** (500 MHz, $CDCl_3$, r.t., ppm) δ: 9.01 (d, $J$ = 9 Hz, 1 H, CH), 8.86 (d, $J$ = 7 Hz, 1 H, CH), 8.81 (d, $J$ = 7 Hz, 1 H, CH), 8.14 (d, $J$ = 9 Hz, 1 H, CH), 8.13 (d, $J$ = 7.5 Hz, 1 H, CH), 8.07 (d, $J$ = 9 Hz, 1 H, CH), 7.94 (dd, $J$ = 8 Hz, 1 H, CH), 7.94 (d, $J$ = 7 Hz, 1 H, CH), 7.85 (dd, $J$ = 8 Hz, 1 H, CH), 7.53 (d, $J$ = 9 Hz, 1 H, CH), 7.46–7.43 (m, 2 H, CH), 7.30–7.26 (m, 4 H, CH, overlaps with signal from $CDCl_3$), 7.16-7.12 (m, 2 H, CH), 4.02 (t, $J$ = 7 Hz, 2 H, $CH_2$), 3.48 (t, $J$ = 7 Hz, 2 H, $CH_2$), 2.49 (s, 3 H, $CH_3$), 2.37 (s, 3 H, $CH_3$), 2.34 (m, 2 H, $CH_2$).

**$^{13}$C{$^1$H} NMR** (125 MHz, $CDCl_3$, r.t., ppm) δ: 145.3 ($C_q$), 140.8 ($C_q$), 140.7 ($C_q$), 2 x 138.4 ($C_q$), 136.9 ($C_q$), 132.4 ($C_q$), 131.9 ($C_q$), 2 x 131.5 (CH), 2 x 131.4 (CH), 131.2 ($C_q$), 130.9 ($C_q$), 2 x 129.3 (CH), 2 x 129.2(CH), 128.9 ($C_q$), 128.8 (CH), 128.0 ($C_q$), 127.7 ($C_q$), 127.3 ($C_q$), 126.8 (CH), 2 x 126.7 (CH), 126.6 (CH), 126.48 ($C_q$), 126.46 (CH), 126.3 ($C_q$), 126.1 (CH), 124.9 ($C_q$), 124.8 (CH), 124.6 ($C_q$), 121.0 ($C_q$), 120.6 (CH), 120.5 (CH), 120.0 ($C_q$), 97.2 ($C_q$), 88.5 ($C_q$), 39.5 ($CH_2$), 34.1 ($CH_2$), 26.6 ($CH_2$), 21.7 ($CH_3$), 21.6 ($CH_3$).

**Elem. Anal. Calc.** (%) for $C_{45}H_{30}$: C 94.70, H 5.30; found: C 94.72, H, 5.43

**HRMS** (APCI$^+$) [$C_{45}H_{30}$ + $H^+$] calc.: m/z = 571.2420. Found m/z = 571.2415 (|Δ| = 0.87 ppm)

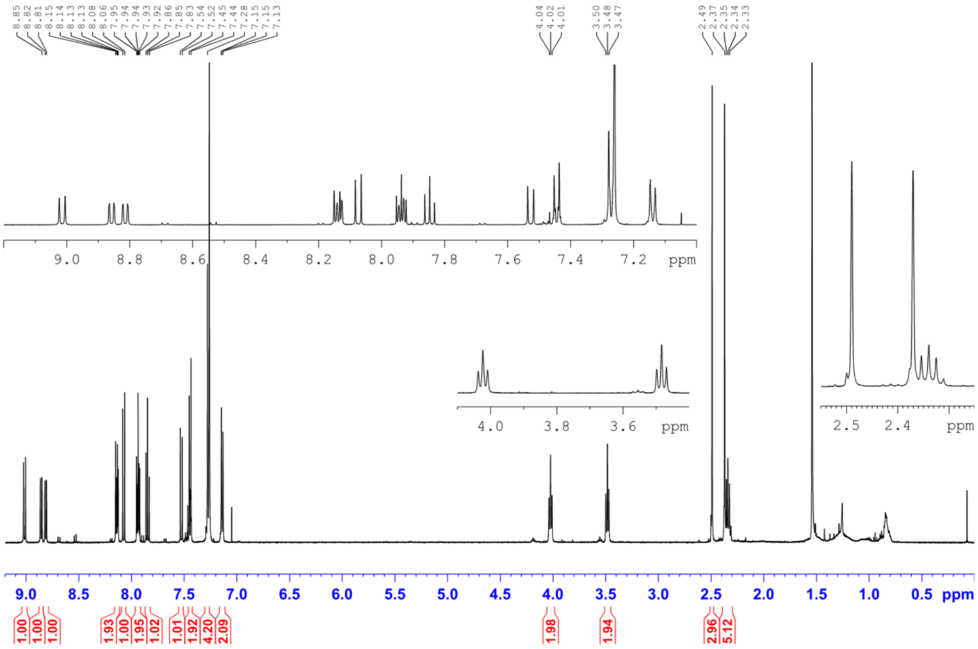

**Figure S14.** $^{1}$H NMR spectrum (500 MHz, $CDCl_3$) of Me-BZ-Me+P.

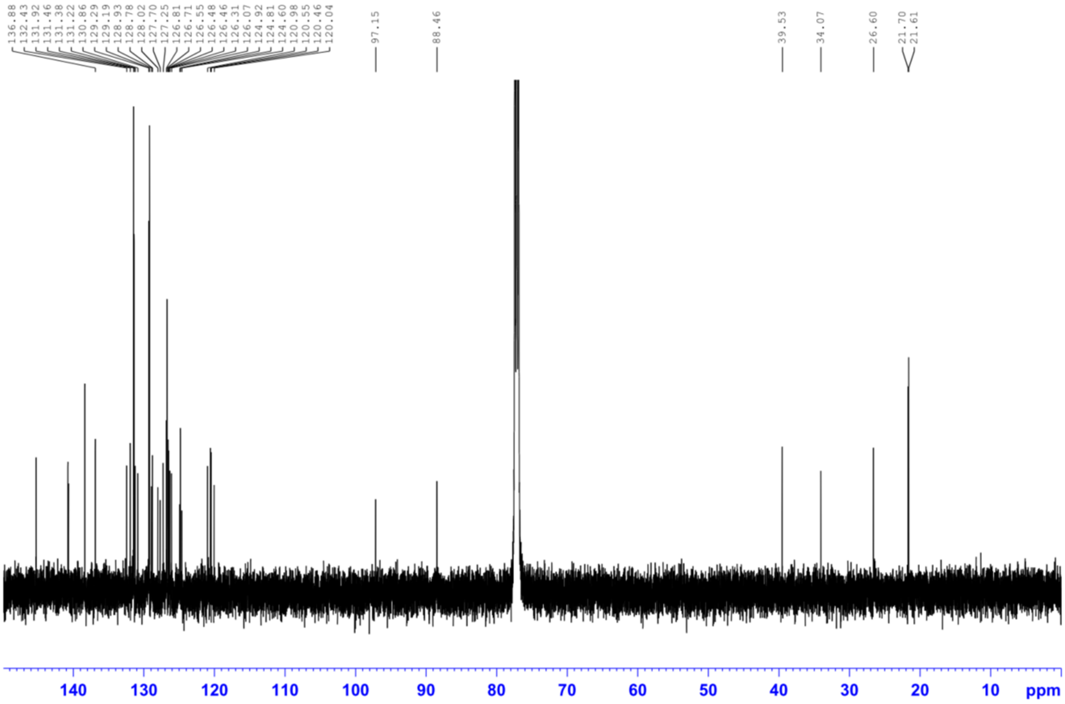

**Figure S15.** $^{13}C\{^{1}H\}$ NMR spectrum (125 MHz, $CDCl_3$) of Me-BZ-Me+P.

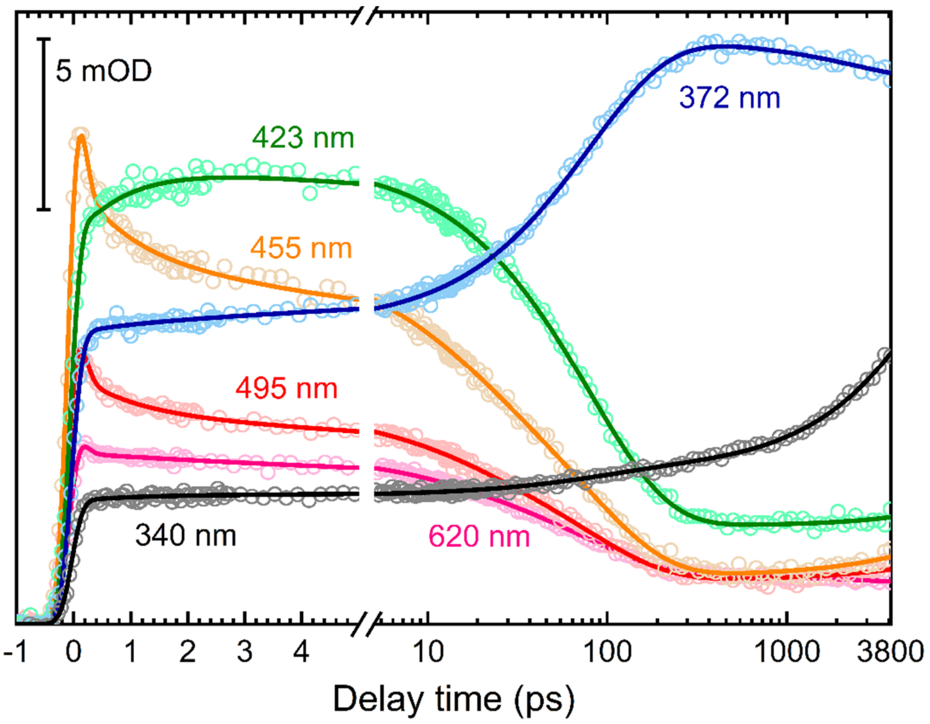

**Figure S16. Target analysis and time traces for perylene trapping reaction.** Data (symbols) are shown for a mixture of Me-BD-Me and perylene in $CHCl_3$ fitted by target analysis (solid lines) at several selected wavelengths.

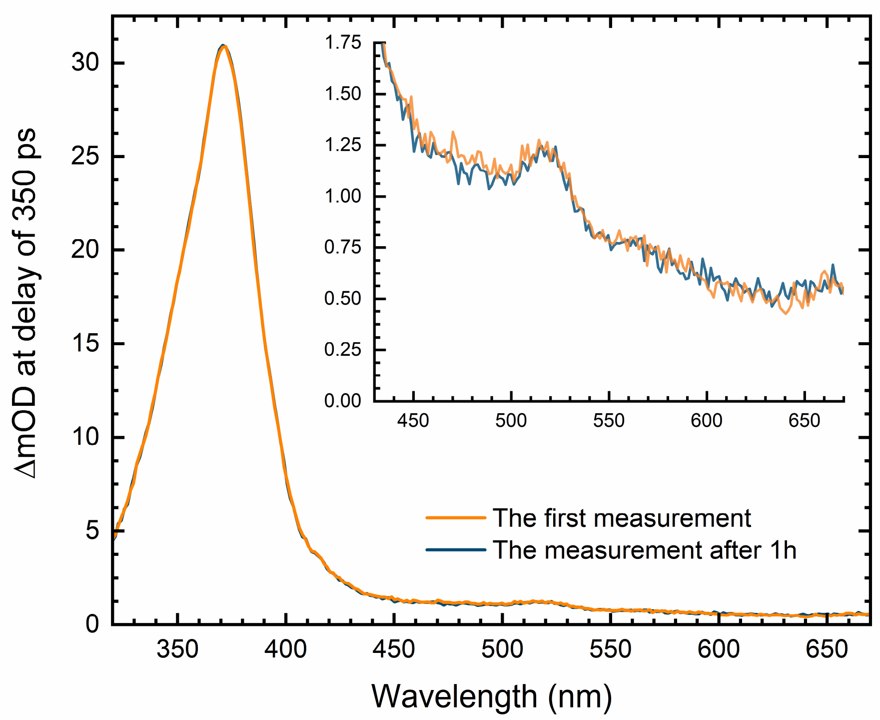

**Figure S17. Comparison of measured transient absorption spectra (at the delay of 350 ps) of Me-BD-Me in $CH_3CN$ in a long-term measurement.** The first measured spectrum (orange line) and the spectrum after 1 h of illumination (blue line) with a 295 nm pump beam are displayed together with an expansion of the spectra in the 430–670 nm region as an inset.